Numerical Evaluation of Low-Speed Impact Behaviour of a Fabric Layered Composite Plate in an Industrial context

Sylvain Treutenaere[1], Franck Lauro[1], Bruno Bennani[1], Grégory Haugou[1], Weijiang Xu[2], Tsukatada Matsumoto[3], Ernesto Mottola[3],Yann-Claude Ngueveu[3]

[1]UVHC, LAMIH, UMR CNRS 8520, 59313 Valenciennes, France
[2]UVHC, IEMN DOAE, UMR CNRS 8201, 59313 Valenciennes, France
[3]TOYOTA MOTOR EUROPE, 1140 Brussels, Belgium

1 Introduction

The use of carbon fabric layered composite in the automotive industry increased very significantly due to their high specific stiffness and strength, their great energy absorption as well as the simplified manufacturing with the use of shapeable and manipulable preforms.
The behaviour understanding and modelling of these materials become essential for their implementation into the design loop, needed for the deployment on mass-produced vehicles. In order to ensure the protection of pedestrians and drivers/passengers in case of collision with a fabric layered composite panel, an accurate and efficient material model dedicated to the finite element analysis of impacts is needed.
The nonlinear material behaviour which leads to differences in the impact response of composites is attributed to fibre failure, intra- and interlaminar matrix cracking, fibre-matrix debonding and strain rate sensitivity of the matrix. Additionally, the textile composite materials are capable of large shearing prior to the ultimate failure due to the sliding and reorientation of yarns. The modelling of all these phenomena is essential to describe the impact behaviour of layered fabric composites.
The intralaminar matrix damage model relies on a close version [1] of the Onera Damage Model proposed by Marcin [2] based on the Continuum Damage Mechanic model proposed by Chaboche [3]. The strain-rate sensitivity is introduced by a coupling between the intralaminar matrix damage model and a rheological viscoelastic model: the generalised Maxwell model. Lastly, a maximum strain criterion and a smeared crack approach are used to model the fibre failure.
The consideration of the interlaminar damage in finite element analysis is nowadays a challenge. The classical framework is to use cohesive elements in the ply interface layers. However this method is time-consuming, breaks the ongoing mesh standards in automotive industry, and does not allow dependence between the intralaminar and the interlaminar damages. Another solution is to recompute a realistic strain distribution within the material model. Kim and Cho [4] have proposed a zig-zag formulation with five degrees of freedom and which takes into account interfacial imperfections. By ensuring an energy balancing between this formulation and the formulation used by the element, it is possible to recover a realistic displacement field through the thickness of the layered materials [5,6]. This theory has been implemented through the user material subroutine interface in LS-Dyna.
The present model is finally used to predict the behaviour and the damage of an industrial structure submitted to impact-type loading. The damage is compared with regard to the experimental one mapped by means of a 3D reconstruction of the matrix damage thanks to precise ultrasonic inspections.

2 Investigated material

The investigated material is issue from a potential non-structural component dedicated to the automotive sector. The considered laminated composite structure is made up with 12K woven fabric for the lower ply, non-crimp fabric for the two internal plies and 3K woven fabric for the upper ply (Fig.1). The matrix is a thermoset epoxy resin.
For the needs of this work, the behaviour of the various composite preforms (NCF, 3K woven or 12K woven) had to be independently investigated. Therefore layered composite plates made up with single preform have been manufactured in order to identify their own behavior.

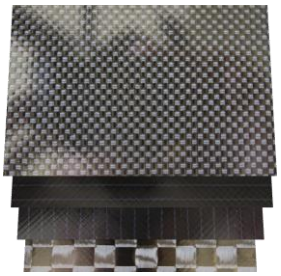

Fig.1: Overview of the preform sequence inside the considered laminated structure: [(0°/90°)^{12K}, (+45°,−45°)^{NCF}, (−45°, +45°)^{NCF,} (0°/90°)^{3K}].

3 Intralaminar behavior model

In this work, the intralaminar damageable viscoelastic model for fabric layered reinforced polymers is formulated in the total Lagrangian framework in order to preserve the material objectivity during the Finite Element Analysis (FEA). The constitutive relation is defined between the Green-Lagrange strain tensor E and the second Piola-Kirchhoff stress tensor S.

3.1 Strain rate sensitivity

The strain rate sensitivity due to the viscoelastic behaviour of the matrix material is introduced by using the general Maxwell model. This model is computationally efficient thanks to the explicit relation between the input strain and the required stress in FEA. The relation is given by the following equation by using Prony's series

$$S = S^{\infty} + \sum_{j=1}^{N} l_j \tag{1}$$

with S^{∞} the long-term stress tensor. l_j is the stress tensor of the jth viscous mechanism among N and is given by

$$l_j = \int_{-\infty}^{t} \boldsymbol{C}_j \cdot \exp\left(-\frac{t-\xi}{\tau_j}\right) : \frac{\mathrm{d}\, E^h(\xi)}{\mathrm{d}\,\xi} \mathrm{d}\,\xi \tag{2}$$

where $\boldsymbol{C}_j$ is the jth viscoelastic stiffness tensor and E^r the driving strain depending on the damage.

3.2 Intralaminar damage model

Experimentally the matrix or fibre cracks are observed to be oriented in the directions of reinforcement or transverse to them. As the Onera Damage Model MicroStructure (ODM_MS) [2] is based on this assumption, the present model [1] relies on a close version of the ODM_MS.

3.2.1 Long-term stress

The long-term stress of the generalised Maxwell model is then defined as follows

$$S^{\infty} = \tilde{\boldsymbol{C}} : (E - E^0) - \boldsymbol{C}^f : (E^r + E^s - E^0) = \tilde{\boldsymbol{C}} : E^h \tag{3}$$

where $\boldsymbol{C}^f$ is the effective stiffness tensor due to only the fibre failure and $\tilde{\boldsymbol{C}}$ is the effective stiffness tensor.

The stored strains E^s are representative of the position oft he crack lips. The stored strains are function of the friction mechanisms, are needed in order to avoid the discontinuity of the response for bi-axial loading, and allow the recovery of the initial stiffness after the damage deactivation.

The evolution of the residual strains E^r is linearly dependent on the damage evolution.
Therefore, the driving strain is given by

$$E^h = E - E^0 - \tilde{\boldsymbol{C}}^{-1} : \boldsymbol{C}^f : (E^r + E^s - E^0) \tag{4}$$

3.2.2 Effective stiffness tensors

The damage is introduced by adding additional compliance to the initial compliance tensor $\boldsymbol{S}^0$. The effective stiffness tensors are thus defined with

$$(\widetilde{\boldsymbol{C}})^{-1} = \boldsymbol{S}^0 + \Delta\boldsymbol{S}^{\boldsymbol{m}} + \Delta\boldsymbol{S}^{\boldsymbol{f}} \text{ and } (\widetilde{\boldsymbol{C}}^{\boldsymbol{f}})^{-1} = \boldsymbol{S}^0 + \Delta\boldsymbol{S}^{\boldsymbol{f}}. \quad (5)$$

The additional compliance tensor due to the matrix damage is given by

$$\Delta\boldsymbol{S}^{\boldsymbol{m}} = \sum_i^3 \eta_i^m d_i^m \boldsymbol{H}_{\boldsymbol{i}}^{\boldsymbol{m}} \quad (6)$$

where $\boldsymbol{H}_{\boldsymbol{i}}^{\boldsymbol{m}}$ is the compliance tensor associated with the matrix damage variable d_i^m. η_i^m represents the crack closure index which varies from 0 (closed crack) to 1 (opened crack).
The same form is used for the fibre damage, however the cracks cannot close:

$$\Delta\boldsymbol{S}^{\boldsymbol{f}} = \sum_i^2 d_i^f \boldsymbol{H}_{\boldsymbol{i}}^{\boldsymbol{f}} \quad (7)$$

where $\boldsymbol{H}_{\boldsymbol{i}}^{\boldsymbol{f}}$ is the compliance tensor associated with the fibre damage variable d_i^f.

3.3 Parameter identification

The parameter identification is carried out by using standard tests on fibre reinforced materials which industries already use. The parameters are determined independently for each preform by using individual specimens.
The elastic and fibre failure parameters are determined by means of tensile and compressive tests in the fibre direction. The matrix damage parameters are coming from cyclic tensile tests at 45° according to the matrix direction. Finally the viscoelastic parameters are obtained throughout Dynamic Mechanical Analysis tests.

4 Recomputation of the strain distribution for layered materials

Due to the industrial environment of this research project, one of the technical and scientific locks was to introduce delamination without changing the existing computer-aided-design process. Since the investigated components are flat and thin, the part is meshed by using shell elements.
Common shell element formulations in LS-Dyna use First-order Shear Deformation Theory (FSDT) with correction factor. This theory leads to inaccurate transverse shear distribution through the thickness of a layered material. It is therefore impossible to predict eventual interlaminar damages and their effects on the transverse shear thickness of the plate.
Kim and Cho [4] have developed a higher order zigzag theory with interfacial imperfections which requires only five degrees of freedom to take into account the delamination effects. Through least square approximation, Kim et al. [5,6] have proposed a methodology to ensure the energy equivalence between this formulation and the Mindlin-Reissner Theory (FSDT), called Enhanced First-Order Shear Deformation Theory.
However this methodology is used during the pre-processing phase to compute an effective transverse shear modulus and the associated shear correction factor. This a priori computation does not allow the study of the damage evolution during a finite element simulation. The equilibrium balance and the determination of the displacement field based on the EFSDT have been integrated in the user material subroutine for accurate simulations of impacts on layered plates.

4.1 Displacement theory

Note: The Greek indices take values of 1 or 2, $\delta_{\alpha\beta}$ is the Kronecker symbol and $H(\bullet)$ is the Heaviside function.
The higher-order zigzag displacement field is given by

$$u_\alpha = u_\alpha^0 - u_{3,\alpha}^0 x_3 + \Phi_{\alpha\beta}\phi_\beta + \sum_{d=1}^{D} \overline{u}_\alpha^{(d)} H(x_3 - x_3^{(d)}) \text{ and } u_3 = u_3^0. \quad (8)$$

The u^0 variables represent the displacements of a point on the reference plane at the position $\Omega \in [-1;1]$ and

$$\Phi_{\alpha\beta} = \left(x_3^3 - \frac{3h^2}{4} x_3 \right) \delta_{\alpha\beta} + \sum_{k=1}^{N-1} a_{\alpha\beta}^{(k)} \left(-\frac{x_3}{2} - \frac{x_3^2}{2h} + (x_3 - x_3^{(k)}) H(x_3 - x_3^{(k)}) \right) \tag{9}$$

with $a^{(k)}$ a coefficient which represents the change of slope at the k-th interface.

$\bar{u}^{(d)}$ is the displacement jump due to the delamination at the interface (d) and is defined by

$$\bar{u}_\alpha^{(d)} = R_{\alpha\beta}^{(d)} \sigma_{\beta 3}^{(d)} \tag{10}$$

with $R^{(d)}$ the compliance of the d-th interface.

Thus, the displacement field can be rewritten

$$u_\alpha = u_\alpha^0 - u_{3,\alpha}^0 x_3 + \Psi_{\alpha\beta} \phi_\beta \tag{11}$$

The newly introduced function Ψ is defined by

$$\Psi_{\alpha\beta} = \Phi_{\alpha\beta} + T_{\alpha\beta} + C_{\alpha\beta}^w \tag{12}$$

with

$$T_{\alpha\beta} = \sum \left(R_{\alpha\gamma}^{(k)} Q_{\gamma\omega}^{s,(k)} \Phi_{\omega\beta,3}(x_3^{(k)}) \right) H(x_3 - x_3^{(k)}) \tag{13}$$

and

$$C_{\alpha\beta}^w = -\frac{1}{h} \int_{-\frac{h}{2}(1+\Omega)}^{\frac{h}{2}(1-\Omega)} (\Phi_{\alpha\beta} + T_{\alpha\beta}) dx_3 \, . \tag{14}$$

C^w is added to make the displacements of the reference plane the variables.

4.2 Energy balance

The Mindlin-Reissner plate theory provides a displacement field defined as follows:

$$v_\alpha = v_\alpha^0 + \theta_\alpha x_3 \, , \tag{15}$$

$$v_3 = v_3^0 \, . \tag{16}$$

This displacement field is considered as the average displacement of the EFSDT through the least square approximation and it leads to the following relationship:

$$v_\alpha^0 = u_\alpha^0 + \int_{-\frac{h}{2}(1+\Omega)}^{\frac{h}{2}(1-\Omega)} (\Psi_{\alpha\beta}) dx_3 \times \phi_\beta \, , \tag{17}$$

$$\theta_\alpha = -u_{3,\alpha}^0 + \frac{12}{h^3} \int_{-\frac{h}{2}(1+\Omega)}^{\frac{h}{2}(1-\Omega)} (x_3 \Psi_{\alpha\beta}) dx_3 \times \phi_\beta \, , \tag{18}$$

$$v_3^0 = u_3^0 \, . \tag{19}$$

Thus, the strain relationship is given by

$$\varepsilon^0 = \gamma^0 - \tilde{\boldsymbol{C}} \kappa_h \, , \tag{20}$$

$$\kappa = \lambda - \tilde{\boldsymbol{\Gamma}}\kappa_h, \tag{21}$$

$$\varepsilon_s^0 = \tilde{\boldsymbol{\Gamma}}_s^{-1}\gamma_s^0. \tag{22}$$

The tensors $\tilde{\boldsymbol{C}}$, $\tilde{\boldsymbol{\Gamma}}$ and $\tilde{\boldsymbol{\Gamma}}_s$ are obtained thanks to an iterative loop which minimizes the difference between the internal energy of the FSDT and of the EFSDT [6].
The displacement field is then recovered by following the equations

$$u_\alpha^0 = v_\alpha^0 - v_{3,\alpha}^0 + \left(\Psi_{\alpha\beta} - \tilde{C}_{\alpha\beta}\right)\tilde{\Gamma}_{\beta\omega}^{-1}\left(\theta_\omega + v_{3,\omega}^0\right) \tag{23}$$

and

$u_3 = v_3^0$.

4.3 Implementation

The classical scheme in LS-Dyna, and by using **`ihyper≠0`** in **`*MAT_USER_DEFINED_MATERIAL`**, provides the deformation gradient as input of the user material subroutine. From that, the Cauchy stress has to be returned (Fig.2).

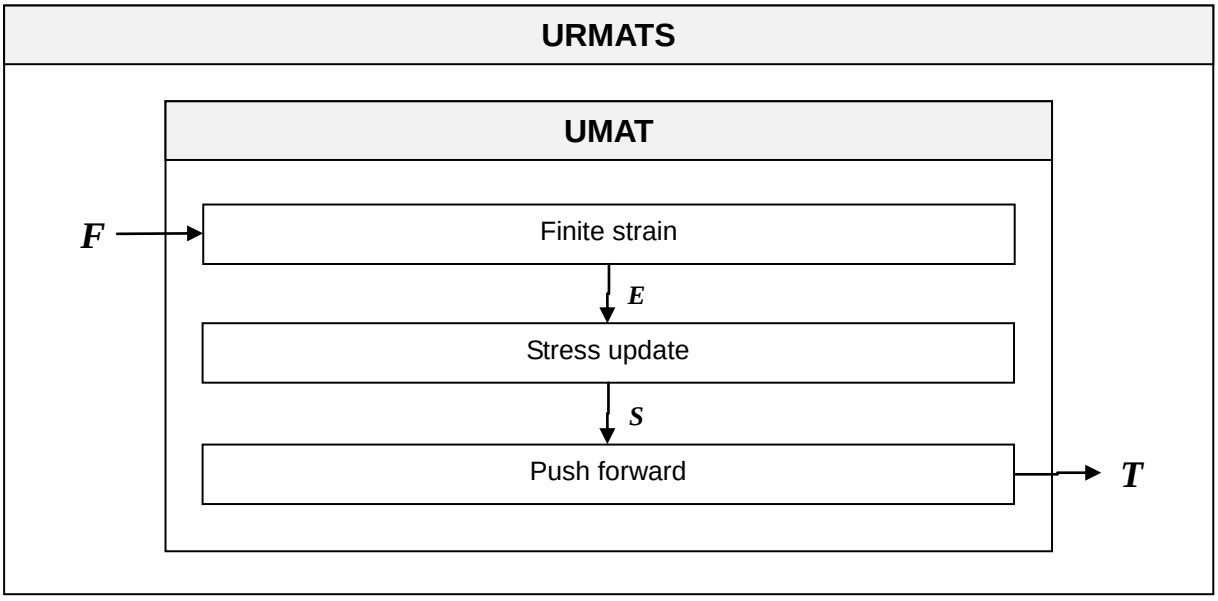

Fig.2: Classical Total Lagrangian UMAT subroutine formulation.

In the case of the present theory, the deformation gradient of the reference plane and the gradient of the deformation gradient of the reference plane are needed as input of the umat subroutine. Thanks to a light modification of the **`urmats`** subroutine (in the dyn21.f file) and by using the **`usrshl_defgrad`** function, these data are passed as input parameters.
For each element and for each new time step the energy balance is achieved. The interlaminar damage is then computed thanks to the stress computation at the interface and these data are stored to be used by the umat subroutine for the next integration points of the element and for the future time steps.
From this, the deformation gradient at the current integration point is computed and the classical algorithm can be recovered (Fig.3).

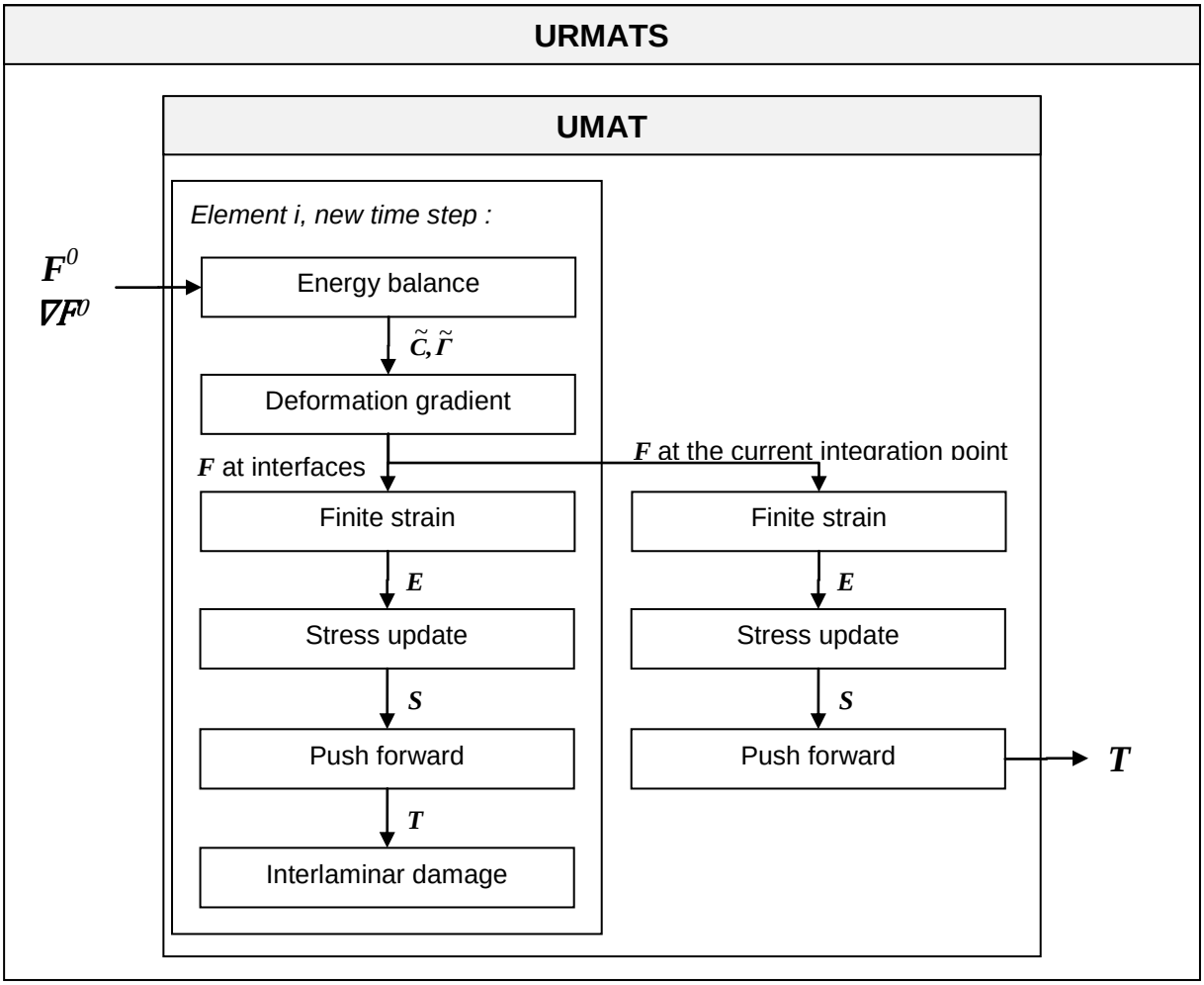

Fig.3: Total Lagrangian UMAT subroutine formulation for layered materials.

4.4 Parameter identification

The parameter identification of the out-of-plane properties and the interlaminar damage model is done by means of standard interlaminar shear tests carried out independently on the different preforms. These tests are in conformity with the standardised interlaminar shear tests in order to be easily reproducible in an industrial framework.
The bending direction influences a lot the damage of the preforms. In case of bending at 45° according to the fibre direction the only damage visible is interlaminar failure. Moreover, the delamination is progressive and the evolution of pure interlaminar damage can be well identified.
Otherwise, in case of bending in the fibre direction, a massive transverse crack occurs through the thickness of the plies. This transverse ply failure leads to a sudden and important loss of bending stiffness. It provides useful information about the intralaminar damage and notably the effect of the transverse shear strains, but also about the intra/interlaminar damage coupling.

4.5 Evaluation of the prediction ability on an industrial component

In order to validate the material model, two types of experimental tests have been carried out on the investigated structure: the standard interlaminar shear tests and a dynamic bulge test in order to approach impact-type loading. Then, and by using exclusively the parameters provided by the identification procedure on the specimens made up with single preforms, numerical simulations have been used to predict the material behavior and the damage, and to evaluate the model. Experimentally, the damage visualisation is carried out by means of C-Scan with a 3-GHz sensor, enabling a resolution of 100 µm.

4.5.1 Standardised interlaminar shear tests

As first validation step, interlaminar shear tests in both 0° and 45° according to the fibre directions are carried out and simulated without parameter adaptation.
The correlation between the numerical and the experimental responses are provided Fig.4 for tests at 0° and Fig.5 for tests with an angle of 45° according to the material direction.

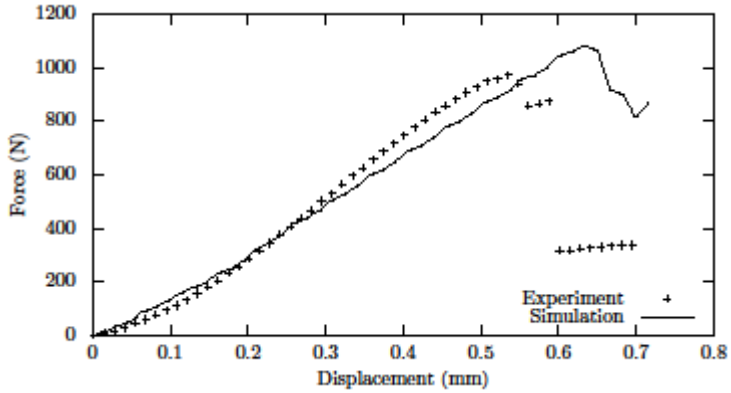

Fig.4: Comparison between the experimental and the predicted numerical responses of transverse shear tests at 0° for the investigated structure.

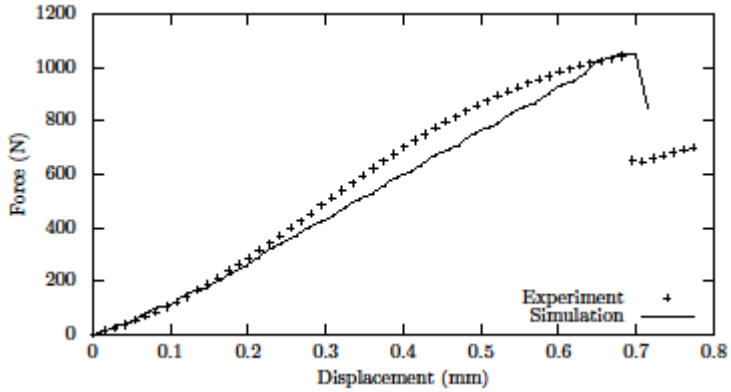

Fig.5: Comparison between the experimental and the predicted numerical responses on transverse shear tests at 45° for the investigated structure.

Compared to the damaged area predicted by finite element analysis (Fig.6 and Fig.8), the real interlaminar damage visualised by mean of ultrasonic measurements (Fig.7 and Fig.9) is located on one interface layer and on one side of the specimen. This is due to the combination of two phenomena. The first one is the approximation of the transverse shear strain field by the actual theory. The second one is the use of a deterministic approach for the numerical simulations. The presence of eventual defects is ignored and leads to an “ideal” behaviour. The introduction of fuzzy variables could lead to a more realistic, but less predictable, behaviour. Otherwise, the progressive and diffuse delamination in the 0° coupon due to plies in the middle oriented at 45° according to the bending and the sudden failures in the 45° coupon, located at different interfaces, are well reported.

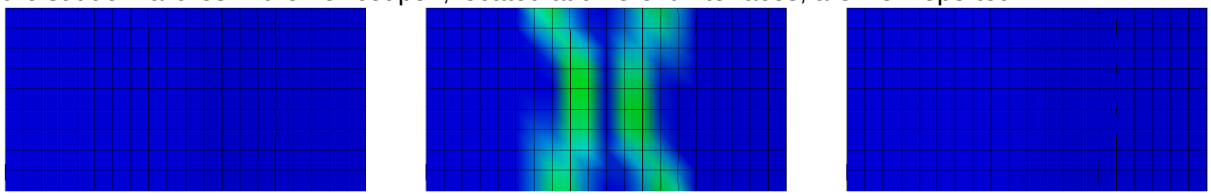

Fig.6: Visualisation of the interlaminar damage predicted by simulation of interlaminar shear tests according to the 0° direction. The three interfaces are given from the lower interface to the upper one (from left to right).

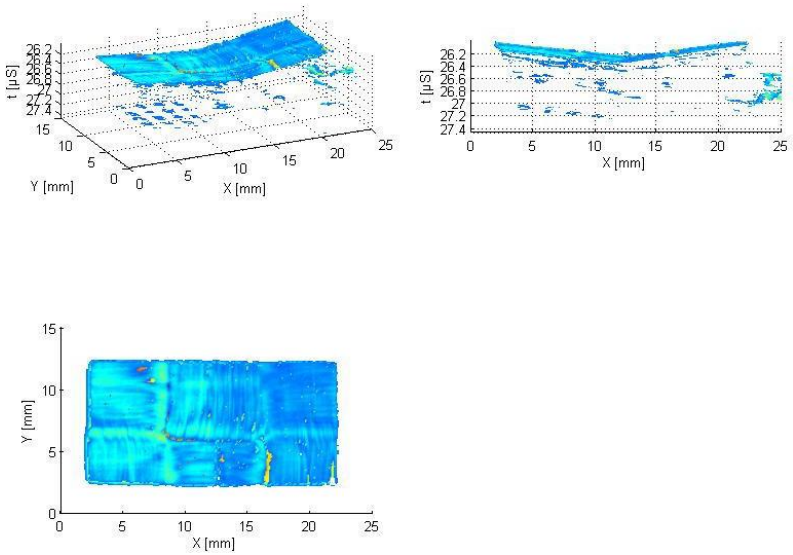

Fig.7: Ultrasonic inspections for damage visualisation on a structure specimen after interlaminar shear tests according to the 0° structure direction.

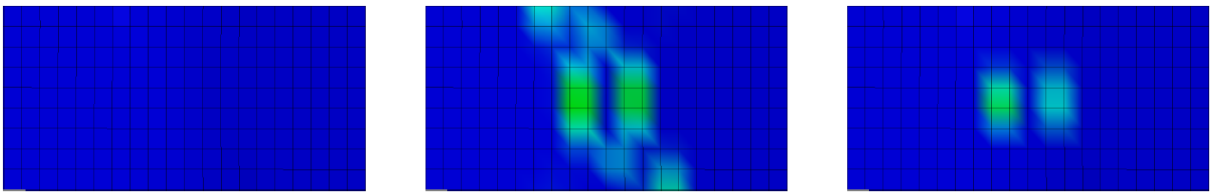

Fig.8: Visualisation of the interlaminar damage predicted by simulation of interlaminar shear tests according to the 45° direction. The three interfaces are given from the lower interface to the upper one (from left to right).

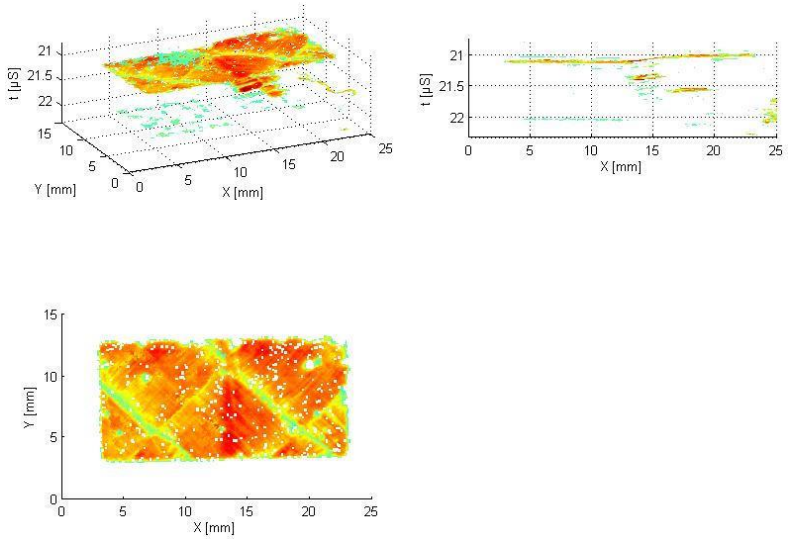

Fig.9: Ultrasonic inspections for damage visualisation on a structure specimen after interlaminar shear tests according to the 45° structure direction.

4.5.2 Controlled impact tests on layered structures

Dynamic bulge tests have been used to approach the low-speed impact loading. Compared to the usual impact tests carried out on fall tower, the bulge tests are carried out on a hydraulic high speed device in order to ensure as much as possible a constant strain rate. Moreover, for a speed loading

less than 300 mm s^{-1}, it is possible to impose a cyclic loading which allows damage controls at given displacements.
Three speed loading have been tested: 1.7 mm s^{-1}, 22 mm s^{-1} and 300 mm s^{-1}. After a first test which leads to the complete failure of the plate, the displacement value when the first fibre failure occurs is imposed as maximal displacement of the pinch. Thus, different plates have been inspected by means of C-scans to evaluate the eventual damage before the first fibre failure.
According to the ultrasonic inspections, the fibre failure of the upper ply is the first damage mechanism which occurs in the plate for the bulge tests. Despite of the transverse shear, no delamination is observed.
Regarding the numerical simulations, the finite element model is presented Fig.10. The shell element formulation which has been used is the Belytschko-Tsay with reduced integration. The shell elements defining the specimen part have a size of 1 mm.

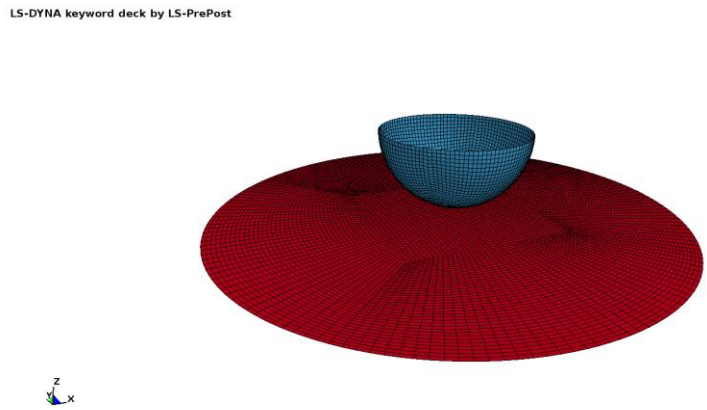

Fig.10: Overview of the model for simulations of bulge tests.

The correlation between the numerical and the experimental responses are provided Fig.11. As recall, the results are predictions of the real behaviour of the plate based on a independent parameter identification of the ply behaviours. The results are encouraging.

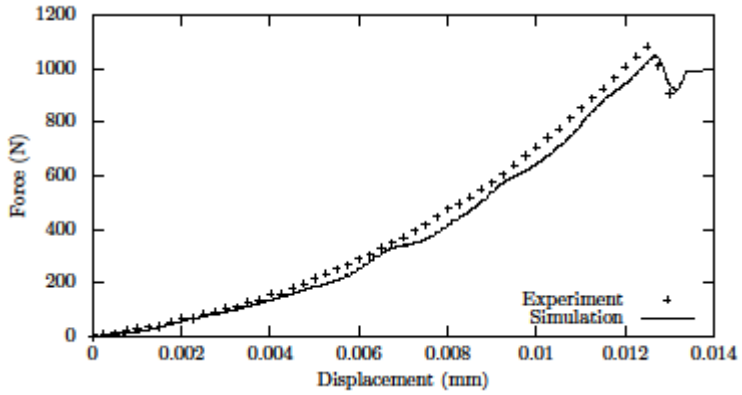

Fig.11: Comparison between the experimental and the predicted numerical responses of bulge test at 300 mms−1 for the investigated structure.

5 Summary

The high specific stiffness and strength, the ease of shaping as well as the great impact performance of layered fabric reinforced polymers encourage their diffusion in the automotive industry. In order to increase the predictability of explicit finite element analysis a material model intended for impact simulations has been developed.
The material model combines the intralaminar behaviour and the effect of delamination without using computationally expensive methods, such as the use of cohesive elements. This allows the use of one

element across the thickness of the laminate and an interaction between intra- and interlaminar damage.
The intralaminar behaviour model is based on the explicit formulation of the matrix damage model developed by the ONERA. Coupling with a Maxwell-Wiechert model, the viscoelasticity is included without losing the direct explicit formulation. The numerical instabilities, due to the strain-softening from the fibre failure, are managed by the smeared-crack approach depending on the element size. Additionally, the intralaminar model is formulated under a total Lagrangian scheme in order to maintain consistency for finite strain by tracking the material direction and by ensuring objectivity.
Thanks to the membrane deformation provided by a Mindlin-Reissner shell formulation and the stacking sequence, the material model is able to compute the through-thickness strains. Based on a higher-order zigzag displacement theory with interfacial imperfections, the strains are established by using an internal loop, which ensures the internal energy equilibrium between both plate theories. The stress at Gauss points are then computed by using the intralaminar model.
This work provides a way to precisely predict the damage and the behaviour of composite plates under impact loading.

6 Acknowledgment

The present research work has been supported by International Campus on Safety and Intermodality in Transportation, the Region Nord Pas de Calais, the European Community, the Délégation Régionale à la Recherche et à la Technologie, the Ministère de l'Enseignement Supérieur et de la Recherche, the Centre National de la Recherche Scientifique and TOYOTA MOTOR EUROPE: the authors gratefully acknowledge the support of these institutions.

7 Literature

[1] TREUTENAERE, S., LAURO, F., BENNANI, B., et al. Modelling of the intralaminar matrix damage with friction effects of fabric reinforced polymers. Composites Part B: Engineering, 2016.
[2] MARCIN, Lionel. Modélisation du comportement, de l'endommagement et de la rupture de matériaux composites à renforts tissés pour le dimensionnement robuste de structures. 2010. Thèse de doctorat. Université Bordeaux 1.
[3] CHABOCHE, J.-L. et MAIRE, J.-F. A new micromechanics based CDM model and its application to CMC's. Aerospace Science and Technology, 2002, vol. 6, no 2, p. 131-145.
[4] KIM, Jun-Sik et CHO, Maenghyo. Efficient higher-order shell theory for laminated composites with multiple delaminations. *AIAA journal*, 2003, vol. 41, no 5, p. 941-950.
[5] KIM, Jun-Sik, OH, Jinho, et CHO, Maenghyo. Efficient analysis of laminated composite and sandwich plates with interfacial imperfections. *Composites Part B: Engineering*, 2011, vol. 42, no 5, p. 1066-1075.
[6] KIM, Jun-Sik et CHO, Maenghyo. Enhanced modeling of laminated and sandwich plates via strain energy transformation. *Composites Science and Technology*, 2006, vol. 66, no 11, p. 1575-1587.